

Experimental Studies on the Erosion Rate of Annealed and Normalised Low Carbon Steel-bank Tubes of Process Boilers

T. S. G. Narayannen¹, Ashish Agarwal² and D. A. Melwin Thomas³

¹Research Scholar, Mechanical Engineering Department, Mewar University Ghaziabad, India

²Associate Professor, Mechanical Engineering Department, IGNOU New Delhi

³Student, Metallurgy Engineering Department, NIT Trichy, E-mail: ashisha@ignou.ac.in

Abstract: The experimental studies are carried out to find the erosion rate of annealed SA192 low carbon steel bank tube and normalized SA 192 low carbon steel bank tube using fly ash particles of different size, velocity impingement angle and feed rate. Erosion rates are evaluated with different impingement angles ranging from 15° to 90°, at four different velocities of 32.5, 35, 37.5 and 40 m/s and four feed rates of 2,4,6, and 8 g/min. The erodent used is fly ash particles of different sizes ranging from 50-250µm of irregular shapes. In all the experimental conditions of fly ash particles it is found that the erosion rate of low carbon steel normalized bank tube is higher than annealed tube.

Keywords: Erosion rate; bank tubes; annealing; normalizing.

1.1. INTRODUCTION

Solid particle erosion may be defined as the removal of material from the surface by the repeated impact of hard and angular particles travelling at considerable velocities. The erosion of metallic tubes in tube banks by particles suspended in gas flows is a serious problem in chemical plants, coal combustion equipment and process when operated in contaminated environments. The damaging effect of erosion substantially reduces the useful life of the tubes. Various ferrous and non-ferrous materials are extensively used in erosive wear situations. Hence solid particle erosion of surface has received considerable attention in the past decades.

2.1. PAST WORK IN EROSION RATE OF MATERIAL

Satyanathan (2001) showed that in M/s. Bharat Heavy Electricals Limited (BHEL) supplied boilers, the fly ash erosion is the major concern for almost one third of total tube failures. The major factors influencing the erosion process are the amount of ash particles, its velocity and the design conditions. Finnie *et al.* (1967) developed analytical model to find the erosion rate based on the assumption that the mechanism of erosion was due to micro cutting. Later it was demonstrated by Levy (1981) that the micro cutting was not the primary mechanism by which ductile structural metal erode. They

conducted experiments and concluded that for ductile material the impacting particles cause severe localized plastic strain, which exceed the strain of material and cause the failure of deformed material, and for brittle materials the energy possessed by erodent particles cause cracking and removal as micro size pieces. Levy (1981) also demonstrated that in ductile materials erosion rate is lowered when its ductility is increased. Misra and Finnie (1981) explained that the number of particles actually striking the surface do not increase the erosion rate in the same way as the number of particles traveling towards the specimen due to the shielding effect provided by the rebounding particles. Levy (1982) tested the same material of specification with different micro structures like fine pearlite and coarse pearlite having different elongation percentage, and found that the erosion rate is less for the material having higher elongation percentage.

Liebhart and Levy (1991) had highlighted that the erosion rates for change in particle size are difficult to explain quantitatively because a number of factors like particle velocity and kinetic energy, number of particles striking the target, interference between the striking and rebounding particles, shape of the particles and the angle of impact of particles are involved. Lyczkowski *et al.* (2002) had stated that the clear understanding of erosion mechanism is essential because erosion is very

serious in the areas of combustion where coal is to be burnt cleanly. Mbabazi *et al.* (2004) had conducted erosion test on mild steel plate with three different fly ash samples from Lethabo, Matimba and Matla power plants at different fly ash velocities and found that experimentally calibrated general model which yielded results that differed by less than 15% from the values measured experimentally. Oka *et al.* (2005a) had stated that material removal is caused by indentation process. It was found that degree of load relaxation depends upon the ability of plastic flow for soft materials. It was concluded that a predictive equation containing material hardness and load relaxation ratio which could be related to find experimental erosion damage data. Oka *et al.* (2005b) had expressed that the mechanical properties of the material can be regarded as the main parameter for estimating erosion damage. Desale *et al.* (2006) had expressed that the surface morphology of the specimen showed deep craters and higher value of average surface roughness for angular particles. Harsha *et al.* (2008) had conducted experiments for ferrous and non ferrous materials to find the erosion rate against the cumulative weight of impinging particles. It was observed that the erosion rate initially increases with increasing cumulative weight of impinging particles and then reaches a steady state value. Wang and Guoyang (2008) had demonstrated that for ductile materials the erosion is caused by the micro cutting and micro ploughing of the erodent particles. For brittle materials like ceramics the energy transfers from erodent material to the specimen. This process induces the material deformation, crack initiation and propagation, and causes removal of material from the specimen surface. Kain *et al.* (2007) studied the failure of low carbon steel tubes considering the SA-210GrA-1 material.

Hutchings and Winter (1974) studied the mechanism of metal removal by impacting the metal targets at an oblique angle by metal balls at velocities up to 250 m/s. They suggested that the initial stage of metal removal is the formation of lip at the exit end of the crater by shearing of the surface layers. Above critical velocity, this lip is detached from the surface by the propagation of ruptures at the base of the lip.

Manish Roy (2006) investigated erosion testing at elevated temperature with special emphasis on

microscopic observation, giving details of the Erosion-Oxidation (E-O) interaction mechanisms and developed Erosion-Oxidation map experimentally for the first time. The influence of various erosion conditions on such a map has been explained on the basis of oxidation characteristics and mechanical properties of the eroding materials, and it has also been inferred that the erosion rate is higher in the oxide erosion regime than in the oxidation-controlled erosion regime, oxidation-affected erosion and metal erosion.

Lindsley and Lewnard (1995) performed a series of tests to determine the erosivity of several different circulating fluidized bed materials. The tests were conducted with 1020 steel as the target material at 400° C and particle velocities of 75 m/sec. The bed material erosivity was found by measuring the sample weight change with time and determining the steady-state erosion rate. It was found that for some conditions, the steel target showed a weight gain owing to soft constituents in the erodent forming a deposit of particle fragments on the surface. Two bed materials were then separated by particle size and each size fraction was erosion tested. The shape of the particles was measured using a quantitative image analysis system and it was found that particle shape changed with the size fraction of the bed particles. Particle composition, which was also found to vary with particle size, was determined using elemental analysis.

Sundararajan and Shewmon (1983) had proposed a correlation between the erosion rate and the thermo-physical properties of the target, for the erosion of metals by particles at normal incidence. This model employed a criterion of critical plastic strain to determine when the material will be removed. Their erosion model (localized model) predicted very well the experimentally observed erosion rates rather than the fatigue-type model.

Jennings *et al.* (1976) have derived mathematical models based on target melting and kinetic energy transfer for predicting ductile target erosion. Dimensional analysis was employed in the development of a mathematical model for predicting the erosion of ductile materials. The basis of the model was an identified erosion mechanism (target melting) and the model was verified in an erosion testing program using three stainless steels, two aluminium alloys, a beryllium copper alloy and

a titanium alloy; the erosive agents were three dusts with hard angular particles and one dust with spherical particles.

Irma Hussainova *et al.* (1999) investigated the surface damage and material removal process during particle-wall collision of the solid particles and hard metal and cermets targets. Targets were impacted with particles over the range of impact velocities (7-50 m/s) at impact angle of 67°. The experimentally observed variations of the coefficient of velocity restitution as a function of the test material properties, impact velocity and hardness ratio were adequately explained by a theoretical model presented by them.

Levy and Foley (1983) studied the erosion behavior of different steel like a plain carbon steel (AISI-SAE 1020), an austenitic stainless steel (type 304) and a low alloy steel (AISI-SAE 4340). The testing was conducted at room temperature using aluminum oxide particles with an average size of 140 microns in an air stream. An attempt was made to characterize the erosion behavior as it relates to the mechanical properties obtainable in these alloys by conventional heat treatments. It was found that the ductility of the steels had a significant effect on their erosion resistance which increased with increasing ductility and that hardness, strength, fracture toughness and impact strength had little effect on erosion behavior.

O'Flynn *et al.* (2001) created a model to predict the solid particle erosion rate of metals and its assessment using heat-treated steels. The model proposed that erosion rate is related to the product of toughness and uniform strain. Two steels (EN 24 and EN 42) were heat treated to form a total of 12 different microstructures, each having distinctly different mechanical behavior. Erosion tests were carried out at a combination of three impact velocities and three angles of particle impingement in a rotating disc accelerator erosion tester. Tensile tests were carried out on all the heat-treated steels over a range of temperatures from room temperature to 400°C. The model predictions were not satisfied by mechanical property measurements made at room temperature. However, for each given erosion test condition, a good linear relationship was found between room temperature erosion rate and $1/(\text{toughness} \times \text{uniform strain})$ when mechanical properties were measured at elevated temperatures. The elevated temperature

chosen to give the best-fit was between 200° and 300°C depending on the impact velocity. It is believed that the significance of the elevated temperature property measurements is that they account for localized heating occurring at the impacting particle during the high strain/strain-rate deformation typical of erosion. Certain heat-treatments gave a poorer fit to the relationship and explanations for this are proffered.

Jianren Fan *et al.* (1992) had conducted an experimental investigation of finned tube erosion processes. It was made by placing erosion prone wax cylinders with fins in a bench-scale cold flow circulating fluidized bed to simulate the long-term erosion effect. A numerical study was conducted for the flow of a dilute particle-laden gas moving past a finned tube undergoing erosion. The results from this study show that the finned tube is a simple and efficient erosion protection method in most industrial two-phase systems where erosion occurs. The fin relative height, the fin number and the angle between two adjacent fins are the three important parameters which affect finned tube erosion protection abilities.

The traditional Eulerian formulation has difficulty in determining the physical properties of the impacting particles, including impact velocity, impact angle and particle number at impact on the wall surface. Lee *et al.* (2002) proposed a new computational procedure for the Eulerian approach to estimate the equivalent Lagrangian solutions for incident and reflected particles near the wall surface. Numerical results of the physical properties of impacting particles using the present Eulerian method show good agreement with those predicted using the Lagrangian method. Comparisons of numerical predictions with reported data show that both approaches are successful in predicting the main feature of the particulate flow near the wall and the erosion rate on the surface, however, the Eulerian approach needs far less computational time than using the Lagrangian approach.

Byeong-Eun Lee *et al.* (2000) concluded from the study that the Eulerian approach as well as the Lagrangian approach can be used in the prediction of solid particle erosion.

Jianren Fan *et al.* (1998) had investigated numerically the finned tube erosion-protection techniques. The numerical results indicate that the

fins fixed on tubes provide a simple and efficient erosion-protection method in most industrial particle-laden systems where erosion occurs.

3.1. MATERIAL REMOVAL (EROSION) MODEL

The mechanical interaction is different for ductile and brittle materials. In the case of ductile materials the impacting particle cause severe, localised plastic strain which is more than the strain to failure of the deformed materials. For brittle materials, the force of erodent particles causes cracking and chipping off of micro size pieces, known as micro cutting (Wang and Guoyang (2008)). This difference is clearly shown in Figure 1.1 (a) & (b).

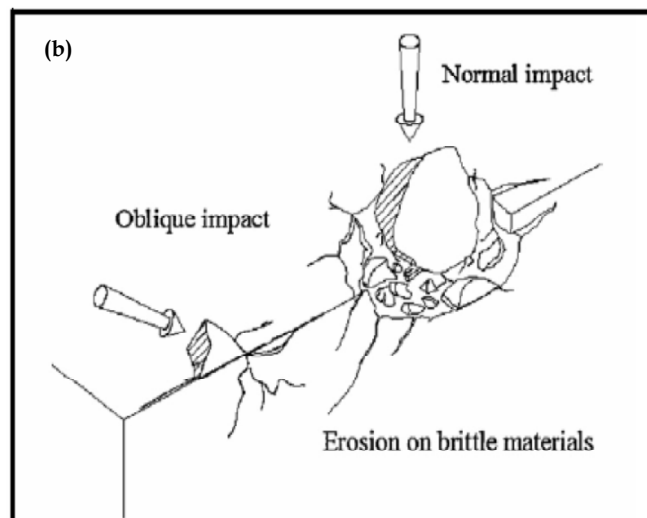
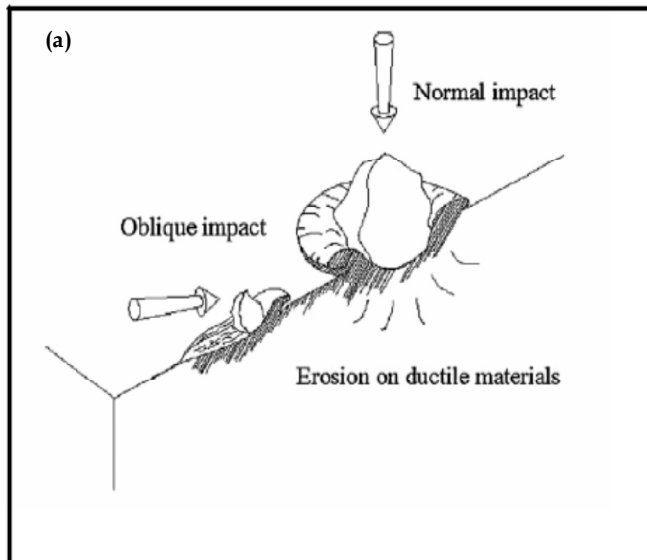


Figure 1.1 (a) & (b): Erosion mechanisms in ductile and brittle material

For ductile material, the erosion mechanism involves sequential plastic deformation process of platelet formation and crater formation due to forging and extrusion. Platelets are initially extruded from shallow craters made by the impacting particle. Once formed, the platelets are forged into a strained condition, in which they are vulnerable to being knocked off the surface in one or several pieces. Owing to the high strain rates, adiabatic shear heating occurs in the surface region immediate to the impact site. Beneath the immediate surface region, a work hardened zone forms, as the kinetic energy of the impacting particles is enough to result in a considerably greater force being imparted to the metal than it is required to generate platelets at the surface. When the surface is completely converted to platelets and craters and the work-hardened zone reaches its stable hardness and thickness, steady state erosion begins. The reason why the steady state erosion rate is the highest is because the subsurface cold-worked zone acts as an anvil, thereby increasing the efficiency of the impacting particles to extrude-forged platelets in the highly strained and most deformable surface region. This cross-section of material moves down through the metal as erosion loss occurs. In the platelet mechanism of erosion, there is a localised sequential extrusion and forging of metal in a ductile manner, leading to removal of the micro segments thus formed. During plastic deformation, the normal component of the particle's kinetic energy is used to extrude-forged the material.

4.1. EXPERIMENTAL SET-UP

The experimental set-up used for the present study is an air jet erosion test rig. The schematic diagram and the photographic view of air jet erosion test rig are shown in Figure 2 respectively. It is owned by research and development lab of M/s. BHEL, Tiruchirappalli, India. The test rig is manufactured as per ASTM G76 standard.

4.2. EXPERIMENTAL PROCEDURE

In this study, tube samples of carbon steel tube material of SA-192 specification, currently in use for bank tubes in almost all power boilers are tested in required conditions at M/s. BHEL's laboratory (recognized by National Accreditation Board for testing and calibration of Laboratories). The tested mechanical properties of tubes of SA-192 materials are given in Tables. I, II, and III

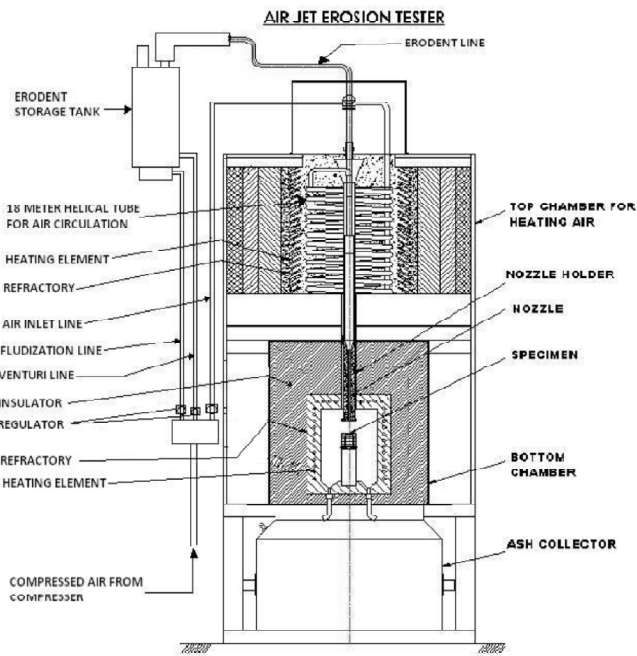


Figure 2.1: Schematic diagram of Air Jet Erosion Test Rig

desired angle using specimen holders. The fly ash is taken in the chamber provided. The velocity and the concentration of fly ash particles are adjusted by controlling the flow of air quantity through the fluidization chamber. A jet of air with the fly ash particles pass through a nozzle and hit the surface of the sample at an angle chosen to place the sample. After doing the experiment for a scheduled time, the sample is removed and it is cleaned and weighed to get the weight loss taken place. The amount of ash used is also measured. The erosion rate is computed as the ratio of loss of weight in grams of test specimen to kilogram of ash particles impinging on the test specimen surface. The erosive rate was evaluated at different impingement angles ranging from 15° to 90°, and at four different velocities of 32.5, 35, 37.5 and 40 m/s.

5.1. RESULTS AND DISCUSSION

5.1.1. Erosion Study on Annealed and Normalized Tube

ASME (American Society of Mechanical Engineers) has permitted the use of the tube having specification SA-192 in boilers. The SA-192 is a low carbon steel tube. The tube having this specification is currently in use for bank tubes in almost all process boilers. For this erosion study tube with annealed heat treatment SA-192 (A) and tube with normalized heat treatment SA-192(N) are selected. The specimen cut from the tubes is the target material and impinging particles are fly ash

5.1.2 Effect of Velocity, Impingement Angle, Feed Rate, Particles Size, Different Fly ash sample and Temperature of Fly Ash Particles on Tube Erosion

Figure 3.1 shows erosion rate at room temperature for annealed and normalized tubes at different impingement velocities ranging from 32.5 m/sec to 40 m/sec and at impingement angle of 30°. The data for graphs are obtained after the steady state of the erosion rate is reached. Erosion rate for normalized tube SA-192(N) is higher than that of annealed SA-192 (A) for a given velocity attributing to ductility and percentage elongation of the materials.

In ductile materials, when fly ash particles impinge with a velocity, at the impact point the particle loses a fraction of its kinetic energy to the

Table I
Shoulder Tensile Test (Test Method: A 370)

S.N.	Reference	Yield Strength (N/mm ²)	Tensile Strength (N/mm ²)	% Elongation on gauge length of 4d
1	Annealed Condition	242	345	37
2	Normalized Condition	291	400	34

Table II
Micro Examination: Test Method ASTM E 407-2 Nos.

S.N.	Details
I	Microstructure shows polygonal grains of ferrite & pearlite typical of Annealed Condition
II	Microstructure shows polygonal grains of ferrite & pearlite typical of Normalized Condition

Table III
Hardness Test: Test Method: ASTM E384

Reference	Hardness in BHN at different locations at test piece		
	Location (1)	Location (2)	Location (3)
Annealed Condition	116	119	116
Normalized Condition	128	125	125

The test specimen was weighed initially and then it was fitted in the jet erosion test rig at a

target material for deformation of the surface and shear strains are induced in the target material. When the shear strain exceeds the elastic limit of the target material, the fly ash particles penetrate the surface of the target material and form platelets, which are removed in the subsequent impingement of the particles. It is the kinetic energy of the fly ash particle that has the greatest effect on the erosion of tubes. The kinetic energy of the fly ash particles is proportional to velocity which causes increase in erosion rate when the velocity of the fly ash particle increases. Since the ductility of the annealed tube is more, the plastic deformation is increased and hence the erosion rate is decreased. So the annealed tube is having less erosion rate.

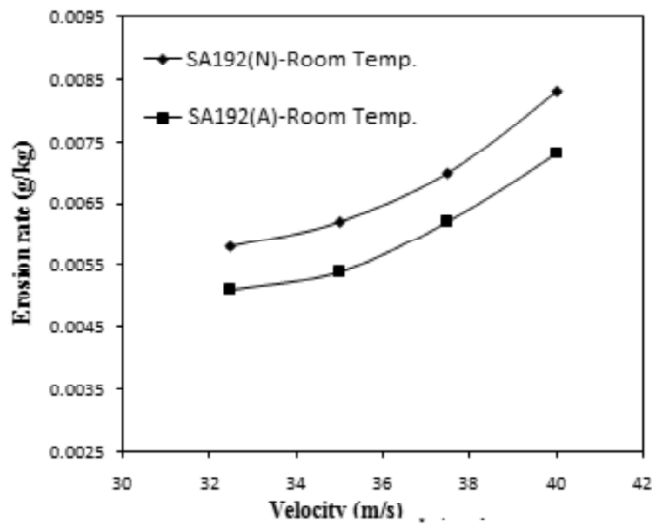


Figure 3.1: Effect of the velocity of fly ash particles on tube erosion -SA-192 (N&A)

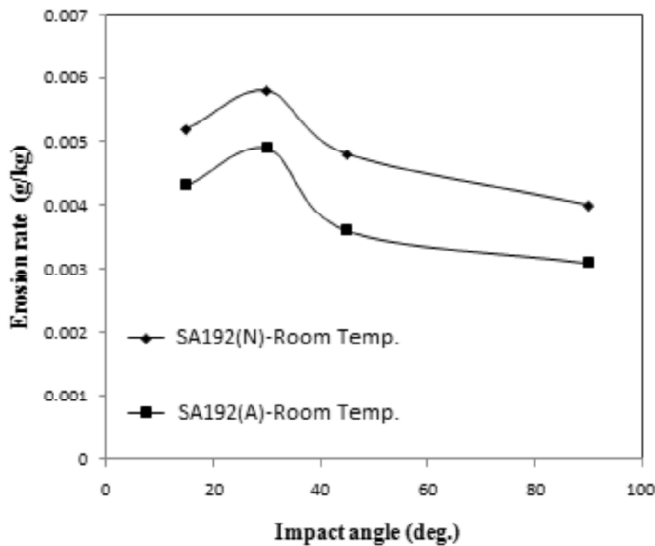


Figure 3.2: Effect of impingement angle on tube erosion-SA-192(N&A)

Figure 3.2 shows the experimental results that are obtained by varying the impingement angles ranging from 15° to 90° at a velocity of 32.5 m/sec at room temperature. The erosion rate increases with the increase in impingement angle initially then decreases with the increase in angle. At about an angle of 30°, the erosion rate is found to be maximum. This could be due to the increase in depth of penetration of the fly ash particle into the target material when the impact angle is increased. When depth of penetration of the particle is increased, the plastic deformation in the target material is increased and thus the erosion rate is reduced. For the same fly ash particles and impingement angle, the erosion rate is mainly a function of target material properties. Also it is clear from Figure 3.2 that erosion rate of SA-192 (A) is nearly 20% less than that of SA-192 (N). Figure 3.3 shows the erosion rate of the specimen for different particle size at room temperature at a velocity of 32.5 m/s and at impingement angle of 30°. The erosion rate increases with the increase in particle size from 50 μm to 125 μm and beyond this size there is no significant increase in erosion rate. More or less constant erosion rate with particle diameter above 125 μm is possible due to the combination of relation between the particle size, the number of particles striking the surface, its kinetic energy and the interference between incoming and rebounding particles. For particle sizes below 125 μm, the kinetic energy of the particles are low to be as effective in removing material as 125 μm size particles or more. When size of the particles are increased the number of the particles actually striking the surface do not proportionally increase due to the shielding effect provided by the rebounding particles.

Experiments are also conducted with four different feed rates of fly ash particles (2, 4, 6, and 8 g/min) with the constant velocity of 32.5 m/sec and impingement angle of 30°. The results are shown in Figure 3.4. In this experiment the erosion rate of specimen is not calculated for per kg weight of fly ash particles as in previous experiments (Figures 3.1, 3.2 & 3.3). There is no increase in erosion rate for the increase in feed rate of the fly ash particles. At higher feed rate of fly ash particles, there is particle-to-particle interference which reduces the effectiveness of the particle to erode the surface. Due to the particle-to-particle interference, the kinetic energy of the incoming particles gets reduced and

there is a chance for some of the fly ash particles to get deflected by the rebounding particles from the target surface. Figures 3.1, 3.2, 3.3 & 3.4 show that erosion rate of annealed tube is less than the erosion rate of normalized tube.

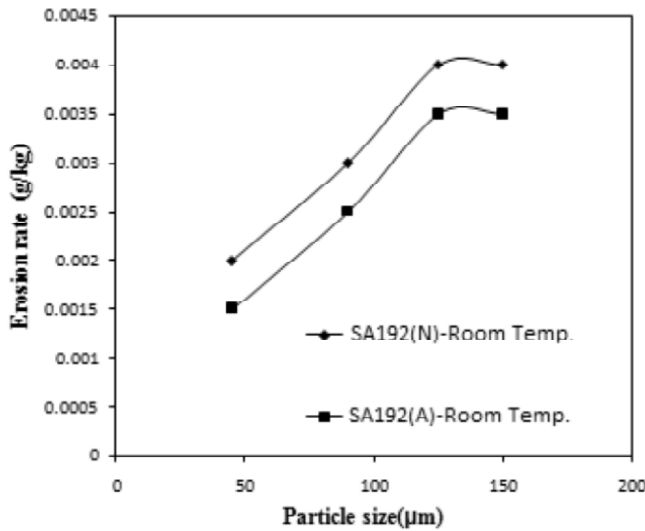


Figure 3.3: Effect of the size of fly ash particles on tube erosion-SA-192 (N&A)

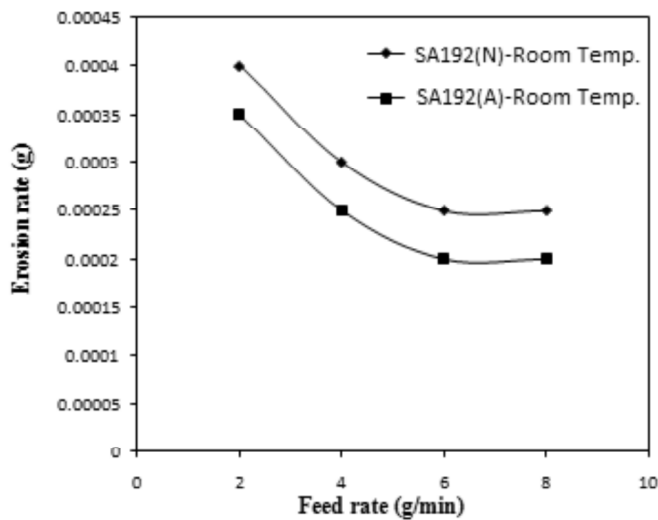


Figure 3.4: Effect of the feed rate of fly ash particles on tube erosion at room temperature-SA-192(N&A)

6.1. CONCLUSION

The experimental investigations confirm that erosion rate of normalized carbon steel tube is more than that of the annealed carbon steel tube. The study also confirms that when the velocity of fly ash particle is increased the erosion rate also increases. If the impingement angle of fly ash particles on the target is increased from 15° to 90°,

5.1.3. Effect of Heat Treatment of the Tubes on Erosion

The erosion is greater in case of normalized material sample. As the normalized material has been cooled in air, it affects the transformation of austenite and affects the microstructure in many ways. There will be less proeutectoid ferrite in normalized hypo eutectoid steels as compared with annealed ones. The faster cooling rate in normalizing will also affect the temperature of the austenite transformation and the fineness of pearlite. In general, faster the cooling rate, the lower the temperature of austenite transformation and finer the pearlite. In normalized tube there is fine lamellar pearlite whereas in annealed tube it is coarse lamellar pearlite which gives normalized steel more strength..than annealed one. The microstructures of annealed and normalized tubes of SA-192 are shown in the Figures which confirm the same.

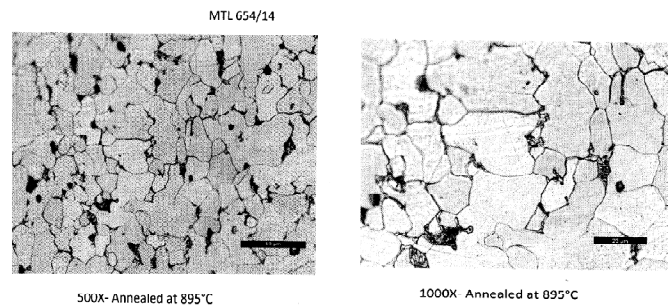


Figure 4.1: Photo Micro graphs of SA 192 (tube) in Annealed Condition

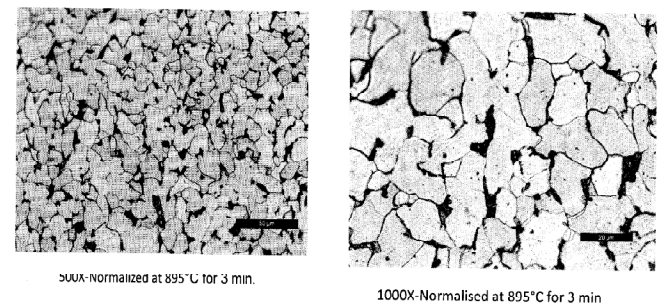


Figure 4.2: Photo Micro graphs of SA 192 (tube) in Normalized Condition

erosion rate reaches at maximum at 30° and then it decreases. It has been observed that erosion rate increases with an increase in the fly ash particle size up to 125µm and beyond that size there is no increase in it. From the experimental results, it is concluded that by using annealed SA-192 tube instead of the normalized SA-192 tube the erosion rate of bank tubes of process boilers can be reduced.

Acknowledgements

The authors thank M/s Bharat Heavy Electricals Limited, Tiruchirappalli, India for their support and encouragements.

References

- [1] Anderson, D. A., J. C. Tannehill and R. H. Pletcher *Computational Fluid Mechanics and Heat Transfer*, 2nd Edition, New York: Hemisphere Publishing co., 1984.
- [2] Bakker, A., A.H. Haidari and L.M. Oshinowo (2001) *Realize greater benefits from CFD*, CEP, AIChE, 45-53.
- [3] Byeong-Eun Lee, C.A.J. Fletcher and M. Behnia (2000) Computational study of solid particle erosion for a single tube in cross flow. *Wear*, 240, 95-99.
- [4] Desale, G. R., B. K. Gandhi and S. C. Jain (2006) Effect of erodent properties on erosion wear of ductile type materials. *Wear*, 261, 914-921.
- [5] Ferziger, J. H. and M. Peric *Computational Methods for fluid dynamics*, New York, Springer Verlag, 1996.
- [6] Finnie, I., J. Wolak and Y. Kabril (1967) Erosion of metals by solid particles. *Jour. matter*, 2, 682-700.
- [7] Haider, A. and O. Levenspiel (1989), Drag coefficient and terminal velocity of spherical and nonspherical particles. *Powder Technology*, 58, 63-70.
- [8] Harsha, A.P., Deepak Kumar Bhaskar (2008) Solid particle erosion behaviour of ferrous and non-ferrous materials and correlation of erosion data with erosion models. *Materials and Design*, 29, 1745-54.
- [9] Hirsch, C *Numerical Computation of Internal and External Flows, volume 2: Computational Methods for Inviscid and Viscous Flows*, John Wiley & Sons, Inc, New-York, 1990.
- [10] Hutchings, I.M. and R.E. Winter (1974) Particle erosion of ductile materials: A Mechanism of Material Removal, *Wear*, 27, 121-128.
- [11] Irma Hussainova, Jakob Kübarsepp and Igor Shcheglov (1999) Investigation of impact of solid particles against hard metal and cermets targets. *Tribology International*, 32, 337-344.
- [12] Jennings, W.H., W.J. Head, and C.R. Mannings Jr, (1976) A mechanistic model for the prediction of ductile erosion. *Wear*, 40, 93.
- [13] Jianren Fan, Dadong Zhou, Keli Z. eng and Kefa Cen (1992) Numerical and experimental erosion protection methods study of finned tube. *Wear*, 152, 1-19.
- [14] Jianren Fan, Ping Sun, Lihua Chen and Kefa Cen (1998) Numerical investigation of a new protection method of the tube erosion by particles impingement. *Wear*, 223, 50-57.
- [15] Jianren Fan, Ping Sun, Youqu Zheng, Xinyu Zhang and Kefa Cen (1999) A numerical study of a protection technique against tube erosion. *Wear*, 225-229, 458-464.
- [16] Jun Yao, Benzhao Zhang and Jianren Fan (2000) An experimental investigation of a new method for protecting bends from erosion in gas-particle flows. *Wear*, 240, 215-222.
- [17] Kain, V., K. Chandra, and B.P. Sharma (2007) Failure of carbon steel tubes in a fluidized bed combustor. *Engg. Failure Anal.*, 15, 182-187.
- [18] Lee, B.E., J.Y. Tu and C.A.J. Fletcher (2002) On numerical modeling of particle-wall impaction in relation to erosion prediction: Eulerian versus Lagrangian method *Wear*, 252, 179-188.
- [19] Levy Alan, V *Solid Particle Erosion and Erosion-Corrosion of Material*, ASM International, Material Park, OH, 1995.
- [20] Levy, A. V. (1982) The erosion of metal alloy and their scales: corrosion erosion wear of materials in emerging fossil energy systems. *Proc. NACE, Berkeley, CA*. 298-396.
- [21] Levy, A. V. (1981) The solid particle erosion behavior of steel as a function of microstructure. *Wear*, 68, 269-287.
- [22] Levy, A. V. and Foley (1983) The erosion of heat treated steels. *Wear*, 91, 45- 64.
- [23] Liebhard, M. and A.J. Levy (1991) The effect of erodent particle characteristics on the erosion metals. *Wear*, 15, 381-390.
- [24] Lindsley and Lewnard (1995) The effect of circulating fluidized bed particle characteristics on erosion of 1020 carbon steel. *Wear*, 188, 33-39.
- [25] Lyczkowski, R. N. and J. X. Bouillard (2002) State-of-the-art review of erosion modeling in fluid/solid systems. *Progress in Energy and Combustion Science*, 28, 543-602.
- [26] Manish Roy (2006) Elevated Temperature Erosive Wear of Metallic Materials. *Jour. Phys. D: Appl. Phys.*, 39, R101-R124.
- [27] Mbabazi, J.G., T.J. Sheer, R. Shandu (2004) A model to predict erosion on mild steel surfaces impacted by boiler fly ash particles. *Wear*, 257, 612-624.
- [28] Misra, A. and E.I. Finnie. (1981) On the size effect in abrasive and erosion wear. *Wear*, 65, No.3, 359-373.
- [29] O'Flynn, M. S., M. S Bingley, A. Bradley and A. J. Burnett (2001) A model to predict the solid particle erosion rate of metals and its assessment using heat-treated steels. *Wear*, 248, 162-177.
- [30] Oka, Y. I. and T. Yoshida (2005a) Practical estimation of erosion damage caused by solid particle impact Part 2: Mechanical properties of materials directly associated with erosion damage. *Wear*, 259, 102-109.
- [31] Oka, Y. I., K. Okamura and T. Yoshida (2005b) Practical estimation of erosion damage caused by solid particle impact Part 1: Effects of impact parameters on a predictive equation. *Wear*, 259, 95-101.
- [32] Sathyanathan, V. T. (2001) BHEL'S experience on pressure parts erosion and corrosion in fossil fuel fired boilers - An overview. Proc. erosion and corrosion prevention in boilers (ECP), NIT, Tiruchirappalli, 7.
- [33] Sundararajan, G. and P. G. Shewmon (1983) A New Model for the Erosion of Metals at Normal Incidence. *Wear*, 84, 237-258.
- [34] Wang, Y. F. and Z. Guoyang (2008), Finite element model of erosive wear on ductile and brittle materials. *Wear*, 265, 871-878.

This document was created with Win2PDF available at <http://www.win2pdf.com>.
The unregistered version of Win2PDF is for evaluation or non-commercial use only.
This page will not be added after purchasing Win2PDF.